EUROFUSION WPS1-PR(16) 16071

L Stephey et al.

Spectroscopic imaging of limiter heat and particle fluxes and the resulting impurity sources during W7-X startup plasmas

Preprint of Paper to be submitted for publication in
21st Topical Conference on High Temperature Plasma
Diagnostics 2016

This work has been carried out within the framework of the EUROfusion Consortium and has received funding from the Euratom research and training programme 2014-2018 under grant agreement No 633053. The views and opinions expressed herein do not necessarily reflect those of the European Commission.

Spectroscopic imaging of limiter heat and particle fluxes and the resulting impurity sources during Wendelstein 7-X startup plasmas[a)]

L. Stephey,[1, b)] G. A. Wurden,[2] O. Schmitz,[1] H. Frerichs,[1] F. Effenberg,[1] C. Biedermann,[3] J. Harris,[4] R. König,[3] P. Kornejew,[3] M. Krychowiak,[3] E. A. Unterberg,[4] and the W7-X team[3, c)]

[1)] *University of Wisconsin - Madison, WI 53706, USA*

[2)] *Los Alamos National Laboratory, NM 87545, USA*

[3)] *Max-Planck-Institut für Plasma Physik, Wendelsteinstrasse 1, 17491 Greifswald, Germany*

[4)] *Oak Ridge National Laboratory, TN 37831, USA*

(Dated: 24 June 2016)

A combined IR and visible camera system[1] and a filterscope system[2] were implemented together to obtain spectroscopic data of limiter and first wall recycling and impurity sources during Wendelstein 7-X startup plasmas. Both systems together provided excellent temporal and spatial spectroscopic resolution of limiter 3. Narrowband interference filters in front of the camera yielded C-III and H_α photon flux, and the filterscope system provided H_α, H_β, He-I, He-II, C-II, and visible Bremsstrahlung data. The filterscopes made additional measurements of several points on the W7-X vacuum vessel to yield wall recycling fluxes. The resulting photon flux from both the visible camera and filterscopes can then be compared to an EMC3-EIRENE synthetic diagnostic[3] to infer both a limiter particle flux and wall particle flux, both of which will ultimately be used to infer the complete particle balance and particle confinement time τ_P.

I. INTRODUCTION

The Wendelstein 7-X stellarator completed its first operational phase (referred to as OP 1.1) in early 2016. During OP 1.1, a set of five poloidal limiters were placed in stellarator symmetric locations on the inboard side of the vacuum vessel in the bean shaped plane. Each limiter was comprised of 9 graphite curved tiles designed to minimize the effects of leading edges and spread the heat and particle load onto a larger surface area. As the limiters were expected to absorb the majority of the power and particle loads, monitoring the limiters was a major diagnostic thrust of OP 1.1. Two limiters were monitored in detail: limiter 3 and limiter 5.

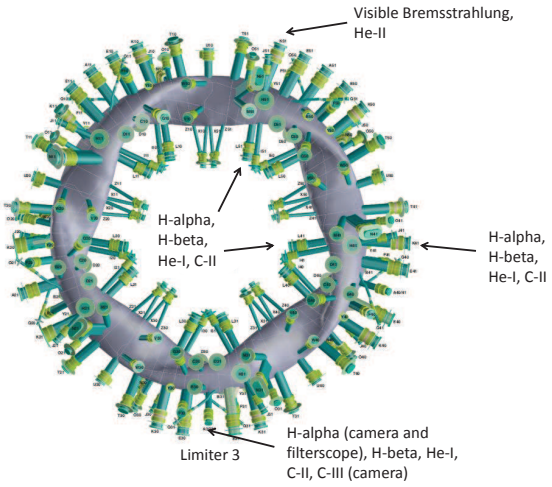

FIG. 1. Location of camera system and filterscope views on W7-X during OP 1.1. Both systems were used to make measurements of limiter 3 (bottom). The types of spectral data obtained at each location are noted.

Limiter 3 was monitored with a LANL combined high-resolution visible-infrared camera system described in this paper and elsewhere[1]. Limiter 3 measurements of H_α, H_β, He-I, and C-II photon flux were also made with an ORNL filterscope system, the details of which are described in[2,4]. Together the combined camera system and the filterscope system provided excellent temporally and spatially resolved spectroscopic measurements of limiter 3. The locations of each measurement are shown in Fig. 1.

Although the limiters were expected to constitute the bulk of the plasma-material interaction, the wall particle flux was also monitored with three additional filterscope channels. Gas fueling particles, high velocity neutrals borne through charge-exchange, and plasma particles advected by cross-field transport can all contribute to a particle flux at the vessel wall.

II. CAMERA SYSTEM

The LANL combined camera system was comprised of a FLIR high-resolution mid-IR camera and an Allied Vision Technology Prosilica 1050 GX visible camera, both of which are also described in[1]. Each camera had ∼1 mm spatial resolution shared a line of sight to limiter 3 tiles 2-6 using a Germanium beamsplitter.

[a)] Contributed paper published as part of the Proceedings of the 21st Topical Conference on High-Temperature Plasma Diagnostics, Madison, Wisconsin, June, 2016.

[b)] Electronic mail: stephey@wisc.edu

[c)] Members of the W7-X Team are listed in H. S. Bosch *et al.*, J. Nucl. Fusion **53** 126001 (2013).

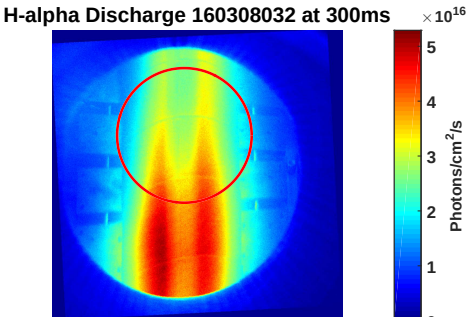

FIG. 2. Representative H_α photon flux data obtained from the visible camera at limiter 3. For reference, the red circle represents the location of the filterscope viewing geometry on the limiter.

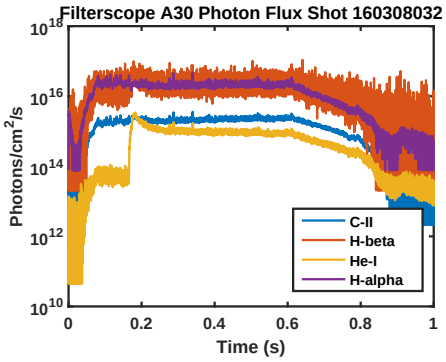

FIG. 3. Representative filterscope data obtained from fiber viewing limiter 3. The filterscope beamsplitter optics allow each spatial channel to be split into four spectral channels. Note that a perturbative He puff can be observed beginning at 200 ms.

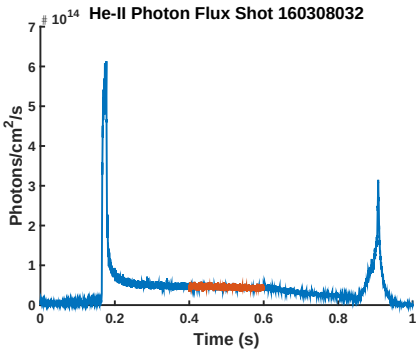

FIG. 4. Representative He-II data for a perturbative helium puff obtained with the filterscope system. The long decay time of the He-II emission (denoted in orange) marks the region used for $\tau^*_{P,He}$ analysis.

The visible camera used the GigE interface standard and data acquisition was controlled by the Matlab Image Acquisition Toolbox. Dual port Ethernet provided a data transfer rate up to 2 Gb/s. The frame rate was 100 Hz at 8 bit color depth and a frame size of 1064 by 1064 pixels with 40% quantum efficiency. The data were uploaded automatically to the W7-X MDSplus system, producing up to 30 GB of data per plasma discharge.

Broadband and narrowband-filtered images of the limiter were obtained with the visible camera. During helium plasmas, a C-III filter was used with a 3 nm FWHM and 70% transmission. During hydrogen plasmas, an H_α filter was used with a 5 nm FWHM and 70% transmission. In both cases two vertical stripes of enhanced photon emission were observed in approximately the same locations as those seen in the infrared[1]. A representative H_α image is shown in Fig. 2.

III. FILTERSCOPE SYSTEM

The ORNL filterscope system is a well-established diagnostic system and has been previously described in detail, so it will not be repeated here[2,4,5]. Rather, the application of the filterscopes as part of an edge diagnostic system at W7-X will be discussed.

The W7-X filterscope system is comprised of 24 Hamamatsu photomultiplier tubes with individually adjustable control voltages and a time resolution of up to 10 microseconds. LabView software controls the data acquisition and populates a local MDSplus tree. An automated python routine was used to copy the local MDSplus tree to the main W7-X MDSplus tree after each plasma discharge.

A narrowband interference filter is placed in front of each photomultiplier to provide measurements of the desired emission line (typically 1-3 nm FWHM). For four views, the light from each fiber is split into four spectral channels with a beamsplitter. These spectral channels were H_α, H_β, He-I, and C-II (representative data are shown in Fig. 3). For the last view, no beamsplitter was used, so either visible Bremsstrahlung or He-II data were obtained. He-II data were especially valuable in measuring the extended decay constant of a perturbative helium puff to infer $\tau^*_{P,He}$ (shown in Fig. 4).

IV. FILTERSCOPE AND CAMERA CALIBRATION

Both the filterscope system and the visible camera were absolutely calibrated to yield measurements of photon flux. A Labsphere model UK2 integrating sphere with known spectral radiance as a function of wavelength was used to calibrate both systems. The transmission of each filter was measured using a Perkin Elmer Lambda 900 spectrophotometer. For the filterscope calibration, neutral density filters were required to prevent the PMTs from saturating. The neutral density transmission curves were also measured and taken into account when building the calibration matrix. For the camera calibration, the opening of the sphere did not completely fill the camera

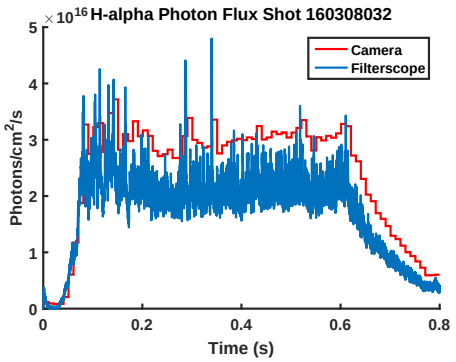

FIG. 5. Visible camera and filterscope H_α data from limiter 3 plotted together for the same discharge. The camera photon flux data within the red circle shown in Fig. 2 were averaged for each image to obtain a photon flux comparable to the filterscope measurement.

image, so a small 40 pixel radius circle in the center of the frame was cropped and used to generate the calibration data.

Both systems were calibrated shortly after the end of OP 1.1. In each case, the actual windows could not be removed from the W7-X vacuum vessel, so identical uncoated quartz (for the filterscope wall views) and sapphire (for the camera and limiter filterscope view) windows were used. Both systems were calibrated with the same data acquisition setup as was used in the experiment. The range of PMT control voltages and exposure times were scanned for the filterscopes and the camera, respectively, to develop a matrix for each system to convert the measured voltages or counts to photon flux.

V. COMBINED SYSTEM

The absolutely calibrated visible camera and filterscope measurements can be combined together to provide well-resolved measurements of limiter 3 both spatially and temporally. To determine the size and location of the filterscope spot on the limiter, the fiber was backlit and photographed and is represented by the red circle shown in Fig. 2. The camera data within this red circle were averaged to produce a timetrace equivalent to the filterscope, shown together in Fig. 5. It should be noted that the measurements differ by roughly 30 percent. This disagreement may stem from several factors, including increased background emission transmitted through the wider camera filter (5 nm vs. 3 nm), the respective differences in detector response and filter blocking in the "out-of-band" wavelength range, and possible small angles between the camera and the interference filter which may lead to increased transmission of additional wavelengths. These differences are still under investigation, as is the determination of the error bars of both measurements.

The interpretation of line-integrated spectroscopic measurements such as these can be relatively complex given that photon emission is a function of the background plasma parameters. For this reason, H. Frerichs has recently developed a synthetic diagnostic module[3] based on EMC3-EIRENE simulations performed by F. Effenberg[6]. This post-processing routine will allow measurements to be compared with simulation results and will allow the local particle fluxes to be extracted along the lines of sight.

VI. SUMMARY AND APPLICATIONS

During OP 1.1 at W7-X, line integrated photon flux measurements have been obtained using the combined camera and filterscope diagnostic. In particular, high fidelity limiter fluxes have been obtained, as well as fluxes at several different wall positions. Using these data, a single reservoir particle balance will be developed to determine the particle confinement time τ_P. Additionally, perturbative helium puff measurements have yielded information about $\tau^*_{P,He}$.

ACKNOWLEDGMENTS

This work was supported in part by the U.S. Department of Energy (DOE) under grants DE-SC0014210, DE-FG02-93ER54222, DE-AC05-00OR22725, DOE LANS Contract DE-AC52 06NA25396, Office of Science DE-SC0014210. The publisher, by accepting the article for publication acknowledges, that the United States Government retains a non-exclusive, paid-up, irrevocable, world-wide license to publish or reproduce the published form of this manuscript, or allow others to do so, for United States Government purposes. This work has been carried out within the framework of the EUROfusion Consortium and has received funding from the Euratom research and training programme 2014-2018 under grant agreement No 633053. The views and opinions expressed herein do not necessarily reflect those of the European Commission.

[1]G. A. Wurden, L. A. Stephey, C. Biedermann, *et al.*, Review of Scientific Instruments (This Conference) (2016).
[2]R. J. Colchin, D. L. Hillis, and R. Maingi, Review of Scientific Instruments **74** (2003).
[3]H. Frerichs, F. Effenberg, O. Schmitz, *et al.*, Review of Scientific Instruments (This Conference) (2016).
[4]E. A. Unterberg, O. Schmitz, D. H. Fehling, *et al.*, Rev. Sci. Instrum. **83** (2012).
[5]N. H. Brooks, R. J. Colchin, D. T. Feling, *et al.*, Rev. Sci. Instrum. **79** (2008).
[6]F. Effenberg, Y. Feng, O. Schmitz, *et al.*, J. Nucl. Fusion **NF-101193 (in review)** (2016).